DOI: 10.1534/genetics.108.090399

Identification and Characterization of Arabidopsis Indole-3-Butyric Acid Response Mutants Defective in Novel Peroxisomal Enzymes

Bethany K. Zolman,*[,1] Naxhiely Martinez,[†] Arthur Millius,[†,2] A. Raquel Adham[†] and Bonnie Bartel[†]

**Department of Biology, University of Missouri, St. Louis, Missouri 63121 and [†]Department of Biochemistry and Cell Biology, Rice University, Houston, Texas 77005*

Manuscript received April 17, 2008
Accepted for publication July 8, 2008

ABSTRACT

Genetic evidence suggests that indole-3-butyric acid (IBA) is converted to the active auxin indole-3-acetic acid (IAA) by removal of two side-chain methylene units in a process similar to fatty acid β-oxidation. Previous studies implicate peroxisomes as the site of IBA metabolism, although the enzymes that act in this process are still being identified. Here, we describe two *IBA-response* mutants, *ibr1* and *ibr10*. Like the previously described *ibr3* mutant, which disrupts a putative peroxisomal acyl-CoA oxidase/dehydrogenase, *ibr1* and *ibr10* display normal IAA responses and defective IBA responses. These defects include reduced root elongation inhibition, decreased lateral root initiation, and reduced IBA-responsive gene expression. However, peroxisomal energy-generating pathways necessary during early seedling development are unaffected in the mutants. Positional cloning of the genes responsible for the mutant defects reveals that *IBR1* encodes a member of the short-chain dehydrogenase/reductase family and that IBR10 resembles enoyl-CoA hydratases/isomerases. Both enzymes contain C-terminal peroxisomal-targeting signals, consistent with IBA metabolism occurring in peroxisomes. We present a model in which IBR3, IBR10, and IBR1 may act sequentially in peroxisomal IBA β-oxidation to IAA.

BECAUSE the auxin indole-3-acetic acid (IAA) orchestrates many aspects of plant growth and development (Woodward and Bartel 2005b), the levels of IAA within a plant must be tightly regulated. In addition to changes in IAA biosynthesis and oxidative degradation, IAA also is transformed into alternate forms, allowing the plant to store IAA until the time and place where active auxin is needed. In one type of storage compound, IAA is conjugated to amino acids or peptides by amide bonds or to sugars by ester bonds; conjugate hydrolases break these bonds to release free IAA (Bartel *et al.* 2001; Woodward and Bartel 2005b). In a second potential storage form, the side chain of the indole moiety is lengthened by two methylene units to make indole-3-butyric acid (IBA), which can be shortened to IAA when necessary (Bartel *et al.* 2001; Woodward and Bartel 2005b).

Although both IBA and certain auxin conjugates have auxin activity in bioassays, genetic experiments suggest that in Arabidopsis this activity does not result from direct effects of the storage compounds, but rather requires release of free IAA from these precursors (Bartel and Fink 1995; Zolman *et al.* 2000). Both IAA conjugates and IBA appear to provide auxin during early Arabidopsis seedling development. In particular, mutants defective in IBA metabolism or IAA-conjugate hydrolysis have fewer lateral roots than wild-type plants, suggesting that the IAA released from storage forms plays a role in lateral root promotion (Zolman *et al.* 2001b; Rampey *et al.* 2004). Different auxin storage forms may have only partially overlapping activity or primarily regulate different physiological responses. For example, mutants with altered IBA responses have stronger rooting defects than IAA-conjugate mutants (Zolman *et al.* 2001b; Rampey *et al.* 2004).

Dedicated enzymes appear to be required to convert auxin storage forms to free IAA. A genetic approach identified a family of Arabidopsis hydrolases showing overlapping specificity in the conversion of various IAA–amino acid conjugates to IAA; mutants defective in each enzyme have altered responses to application of the corresponding conjugates (Bartel and Fink 1995; Davies *et al.* 1999; Rampey *et al.* 2004). We are taking a similar genetic approach to discover the enzymes required for conversion of IBA to IAA.

Even-numbered side-chain-length derivatives of IAA (Fawcett *et al.* 1960) and the synthetic auxin 2,4-dichlorophenoxyacetic acid (2,4-D; Wain and Wightman 1954) possess auxin activity. Wheat and pea extracts shorten these compounds in two-carbon increments (Fawcett *et al.* 1960). These results suggest that IBA,

[1]*Corresponding author:* Department of Biology, University of Missouri, R223 Research Bldg., 1 University Blvd., St. Louis, MO 63121-4400. E-mail: zolmanb@umsl.edu

[2]*Present address:* University of California, San Francisco, CA 94158.

which is structurally identical to IAA but with two additional methylene units on the side chain, and 2,4-dichlorophenoxybutyric acid (2,4-DB), the analogous elongated derivative of 2,4-D, are converted by plants to bioactive IAA and 2,4-D, respectively. The mechanism of this conversion was suggested to be similar to the two-carbon elimination that occurs during fatty acid β-oxidation (Fawcett *et al.* 1960). In this model, IBA acts as a "slow-release" form of IAA (van der Krieken *et al.* 1997), and auxin effects promoted by IBA would be limited by the β-oxidation rate.

To elucidate the proteins necessary for IBA activity, we have isolated Arabidopsis mutants with altered IBA responses. Exogenous IBA inhibits primary root elongation; mutants that cannot sense or respond to IBA have elongated roots on IBA compared to wild type (Zolman *et al.* 2000). *IB*A-*r*esponse (*ibr*) mutants remain sensitive to short-chain auxins (IAA and 2,4-D), whereas general auxin-response mutants defective in auxin signaling, such as *axr2/iaa7* (Timpte *et al.* 1994; Nagpal *et al.* 2000) and *axr3/iaa17* (Leyser *et al.* 1996; Rouse *et al.* 1998), or transport, including *aux1* (Pickett *et al.* 1990; Bennett *et al.* 1996; Marchant *et al.* 1999), display reduced responses to both IBA and IAA (Zolman *et al.* 2000).

Isolation of the genes defective in *ibr* mutants has revealed a close connection between IBA metabolism and peroxisomal function. For example, mutants defective in the peroxins PEX4 (Zolman *et al.* 2005), PEX5 (Zolman *et al.* 2000), PEX6 (Zolman and Bartel 2004), PEX7 (Woodward and Bartel 2005a), and PEX12 (Fan *et al.* 2005) or in the PXA1/CTS1/PED3 transporter (Zolman *et al.* 2001b), which is required for import of peroxisomal substrates (Footitt *et al.* 2002; Hayashi *et al.* 2002; Theodoulou *et al.* 2005), are resistant to IBA. The isolation of IBA-response mutants defective in these factors, coupled with the fact that peroxisomes are the primary site of fatty acid β-oxidation in plants (Graham and Eastmond 2002; Baker *et al.* 2006), implicates peroxisomes as the subcellular location for IBA-to-IAA conversion. Mutants defective in peroxisomal biogenesis likely disrupt IBA responses by compromising the peroxisomal environment or by limiting peroxisomal import of enzymes necessary for IBA β-oxidation. Indeed, these *ibr* mutants display additional phenotypes associated with peroxisome defects, such as sucrose dependence during seedling development due to slowed β-oxidation of seed storage fatty acids (Zolman *et al.* 2000).

Other *ibr* mutants may be defective in enzymes that act in the peroxisome matrix to catalyze the β-oxidation of fatty acids, IBA, or both. In Arabidopsis, at least two genes encode related isozymes for each fatty acid β-oxidation step (Baker *et al.* 2006). Following substrate import into the peroxisome by PXA1, a CoA moiety is added by one of two long-chain acyl-CoA synthetases (LACS; Fulda *et al.* 2002, 2004). One of six acyl-CoA oxidases (ACX) catalyzes the oxidation step, adding a double bond while releasing hydrogen peroxide (Hayashi *et al.* 1999; Hooks *et al.* 1999; Eastmond *et al.* 2000; Froman *et al.* 2000; Rylott *et al.* 2003; Adham *et al.* 2005; Pinfield-Wells *et al.* 2005). Next, a multifunctional protein (MFP2 or AIM1), containing both enoyl-CoA hydratase and acyl-CoA dehydrogenase activity, forms a β-ketoacyl-CoA thioester (Richmond and Bleecker 1999; Eastmond and Graham 2000; Rylott *et al.* 2006). This substrate undergoes a thiolase-mediated retro-Claisen reaction, releasing two carbons as acetyl-CoA and producing a chain-shortened substrate that can reenter the β-oxidation spiral for continued catabolism. *PED1/KAT2* encodes the most highly expressed thiolase in Arabidopsis (Hayashi *et al.* 1998; Germain *et al.* 2001).

We recently described the *ibr3* mutant, which displays defective IBA and 2,4-DB responses but responds normally to other conditions tested (Zolman *et al.* 2007). *IBR3* (*At3g06810*) encodes a putative peroxisomal acyl-CoA dehydrogenase or oxidase that resembles the mammalian ACAD10 and ACAD11 enzymes. Because the *ibr3* mutant does not have apparent fatty acid β-oxidation defects, IBR3 may act in IBA β-oxidation to IAA (Zolman *et al.* 2007). In addition to *ibr3*, mutants defective in several fatty acid β-oxidation enzymes, including *aim1*, *ped1*, and multiple *acx* mutants, show altered responses to exogenous IBA (Zolman *et al.* 2000; Adham *et al.* 2005); whether these IBA-response defects reflect a direct enzymatic role on IBA β-oxidation intermediates or an indirect disruption of IBA-to-IAA conversion remains an open question.

Here, we describe the phenotypic characterization of *ibr1* and *ibr10*, two strong IBA-response mutants that, like *ibr3*, have no apparent defects in peroxisomal fatty acid β-oxidation. We used map-based cloning to demonstrate that *IBR1* and *IBR10* encode a short-chain dehydrogenase/reductase (SDR) family enzyme and a putative enoyl-CoA hydratase/isomerase (ECH), respectively. Both IBR1 and IBR10 have peroxisomal-targeting signals. The specific IBA-response defects of *ibr1* and *ibr10* mutants suggest that IBR1 and IBR10 are needed for the peroxisomal conversion of IBA to IAA.

MATERIALS AND METHODS

Mutant isolation: The *ibr1-1* and *ibr1-2* mutants were described previously as B1 and B19, ethyl methanesulfonate (EMS)-induced IBA-response mutants in the *Arabidopsis thaliana* Columbia (Col-0) background (Zolman *et al.* 2000). Additional screens of various mutagenized populations revealed several new mutants with IBA-resistant root elongation. *ibr1-3*, *ibr1-4*, and *ibr1-5* were isolated from the progeny of Col-0 seed mutagenized by fast-neutron bombardment (Zolman *et al.* 2007). *ibr1-8* was isolated from the progeny of EMS-mutagenized Col-0 seeds (Lehle Seeds, Round Rock, TX). *ibr10-1* was isolated by screening T-DNA insertion lines in the Col-0 accession (pool CS75075; Alonso *et al.* 2003), although our analysis indicated that the T-DNA was not linked to the IBA-resistant phenotype (data not shown). *chy1-3* (Zolman

et al. 2001a) and *ibr3-1* (Zolman *et al.* 2007) were described previously and are Col-0 alleles with point mutations in *CHY1/At5g65940* and *IBR3/At3g06810*, respectively.

The *ibr1-7* (SALK_010364), *hcd1/at4g14440* (SALK_012852), and *echic/at1g65520* (SALK_036386) mutants in the Col-0 accession were from the Salk Institute sequence-indexed insertion collection (Alonso *et al.* 2003). The three insertion mutants were genotyped using PCR amplification with a combination of genomic primers and a modified LBb1 T-DNA primer (5′-CAAACCAGCGTGGACCGCTTGCTGCA-3′; http://signal.salk.edu). The T-DNA position in *ibr1-7* was confirmed by sequencing the amplification product directly.

Higher-order mutants were generated by crossing and were identified using PCR-based genotyping. For *ibr1-2*, amplification with the oligonucleotides T1J24-8 (5′-GAAGCTTTACCTGCAG GAGAAGTATAGAGG-3′) and T1J24-12 (5′-TAAGAGATGTCT TCTGTGTTTTTGGACTCA-3′) yields a 175-bp product with one *Dde*I site in wild type that was absent in *ibr1-2*. For *ibr10-1*, amplification with At4g14430-1 (5′-ATTTGCACAATTCAACAA CAACACGATTTC-3′) and At4g14430-2 (5′-TAGCCCTAAC CAACGCCGAGAAATAATC-3′) yields a 546-bp product in wild type and a 468-bp product in *ibr10-1*. *ibr3-1* was genotyped using a derived cleaved amplified polymorphic sequence marker (Michaels and Amasino 1998; Neff *et al.* 1998) in which amplification with F3E22-22 (5′-ATGGTGCAGTCTTCCAGGG CCTAACCTAGC-3′; altered residue underlined) and F3E22-23 (5′-GTTTTGATGACGCACCTCATGGACATGCTG-3′) yields a 240-bp product with one *Alu*I site in *ibr3-1* that was absent in wild type.

Plant growth and phenotypic characterization: Surface-sterilized seeds were plated on plant nutrient (PN) medium (Haughn and Somerville 1986) solidified with 0.6% (w/v) agar and supplemented with 0.5% sucrose (PNS), hormones, kanamycin, or Basta (glufosinate–ammonium; Crescent Chemical, Augsburg, Germany) as indicated. Plates were incubated under continuous light at 22°; for auxin experiments, plates were placed under yellow filters to slow breakdown of indolic compounds (Stasinopoulos and Hangarter 1990). Seedlings were transferred to soil and grown at 18°–22° under continuous illumination.

Prior to phenotypic analyses, *ibr1-2* and *ibr10-1* were backcrossed to the parental Col-0 accession four and two times, respectively. For root elongation assays, seeds were plated on PNS supplemented with hormones at the indicated concentrations. Roots were measured after 7 or 8 days at 22° under yellow light. For some assays, seeds first were stratified for 3 days in 0.1% agar at 4° and germinated under white light for 2 days at 22° before being moved to assay plates. For lateral root assays, seeds were stratified for 3 days at 4°, grown on PNS for 4 days under yellow light at 22°, and then transferred to PNS supplemented with the indicated hormone and grown for 4 days under yellow light at 22°. To assay sucrose-dependent hypocotyl elongation, seeds were stratified for 3 days at 4° and grown on PN or PNS for 1 day under white light followed by 5 days in the dark at 22°.

ibr10-1 was crossed to Col-0 carrying a DR5-GUS transgene (Guilfoyle 1999). Lines homozygous for DR5-GUS and *ibr10-1* were selected on 12 μg/ml kanamycin and by genotyping as described above. For analysis of DR5-GUS reporter gene activation, seeds were germinated on PNS and grown for 4 days and then transferred to PNS supplemented with auxin for the indicated number of days. Histochemical localization was done by staining homozygous seedlings for 2 days at 37° with 0.5 mg/ml 5-bromo-4-chloro-3-indolyl-β-d-glucuronide (Bartel and Fink 1994).

Positional cloning and mutant complementation: *ibr1* and *ibr10* alleles were outcrossed to Landsberg *erecta tt4* (L*er*) and Wassilewskija accessions for recombination mapping. Mutations were mapped using PCR-based molecular markers (http://www.arabidopsis.org) on DNA from IBA-resistant F_2 plants. *ibr1-8* was identified as an *ibr1* allele on the basis of failure to complement *ibr1-1*. Candidate genes were PCR amplified from mutant DNA and sequenced directly using gene-specific primers.

To make the 35S-*IBR1*c construct, the *Sal*I/*Not*I insert from the 103N7T7 EST (Newman *et al.* 1994) was ligated into the 35SpBARN (Leclere and Bartel 2001) plant transformation vector cut with *Xho*I and *Not*I. An *IBR1* genomic rescue construct was made by digesting the T1J24 bacterial artificial chromosome containing *IBR1* with *Bgl*II, yielding a 4-kb fragment containing the *IBR1* coding sequence plus 1278 bp 5′ and 1118 bp 3′ of the coding region. This fragment was subcloned into the *Bam*HI site of pBluescript KS+ to give pKS-*IBR1*g. An *Eco*RI/*Xba*I fragment was subcloned from pKS-*IBR1*g into the plant transformation vector pBIN19 (Bevan 1984) cut with the same enzymes to give pBIN-*IBR1*g.

For complementation of the *ibr10* mutant, Col-0 DNA was amplified with *PfuTurbo* DNA polymerase (Stratagene, La Jolla, CA) using primers modified to add *Sal*I and *Not*I restriction enzyme sites (added residues underlined): At4g14430-5 (5′-CGT CGACCATAGACCAATCAGGATAAGGTATATTTCTCTC-3′) and At4g14430-6 (5′-GAGGCGGCCGCTGTCTCTTTCTCCCAAAAC ATGTG-3′). The purified PCR product was cloned into the PCR4-Blunt TOPO vector following the manufacturer's instructions (Invitrogen, Carlsbad, CA) to give pTOPO-*IBR10c*. The insert of pTOPO-*IBR10c* was sequenced to ensure the absence of PCR-derived mutations. The *Sal*I/*Not*I fragment from pTOPO-*IBR10c* was subcloned into *Xho*I/N*ot*I-cut 35SpBARN to give 35S-*IBR10*.

Complementation constructs were introduced into *Agrobacterium tumefaciens* GV3101 (Koncz *et al.* 1992) by electroporation (Ausubel *et al.* 1999) and transformed into mutant alleles using the floral dip method (Clough and Bent 1998). Transformed T_1 seedlings and homozygous T_3 lines were identified by selecting seedlings resistant to 7.5 μg/ml glufosinate–ammonium (35S-*IBR1c* and 35S-*IBR10*) or 12 μg/ml kanamycin (pBIN-*IBR1g*).

RESULTS

***ibr1* and *ibr10* have IBA-response phenotypes:** Isolation and characterization of mutants with altered responses is a powerful method for identifying proteins involved in specific metabolic pathways. We screened mutagenized seed pools for mutants with long roots on normally inhibitory IBA concentrations. In addition to two previously described *ibr1* alleles from EMS-mutagenized pools (Zolman *et al.* 2000), we isolated an additional EMS-induced *ibr1* allele, three *ibr1* alleles from a fast-neutron mutagenized population, and a single *ibr10* allele from a T-DNA-mutagenized population (Alonso *et al.* 2003). Both *ibr1* and *ibr10* mutants were resistant to the inhibitory effects of IBA on root elongation (Figure 1A). All of the *ibr1* alleles displayed a similar level of IBA resistance (Figure 1A and data not shown) and we chose *ibr1-2* for more detailed analysis.

We examined IBA-response defects under several conditions, comparing *ibr1* and *ibr10* with the previously described *chy1-3* (Zolman *et al.* 2001a) and *ibr3-1* (Zolman *et al.* 2007) mutants. First, we examined the effects of increasing IBA concentrations on root elongation.

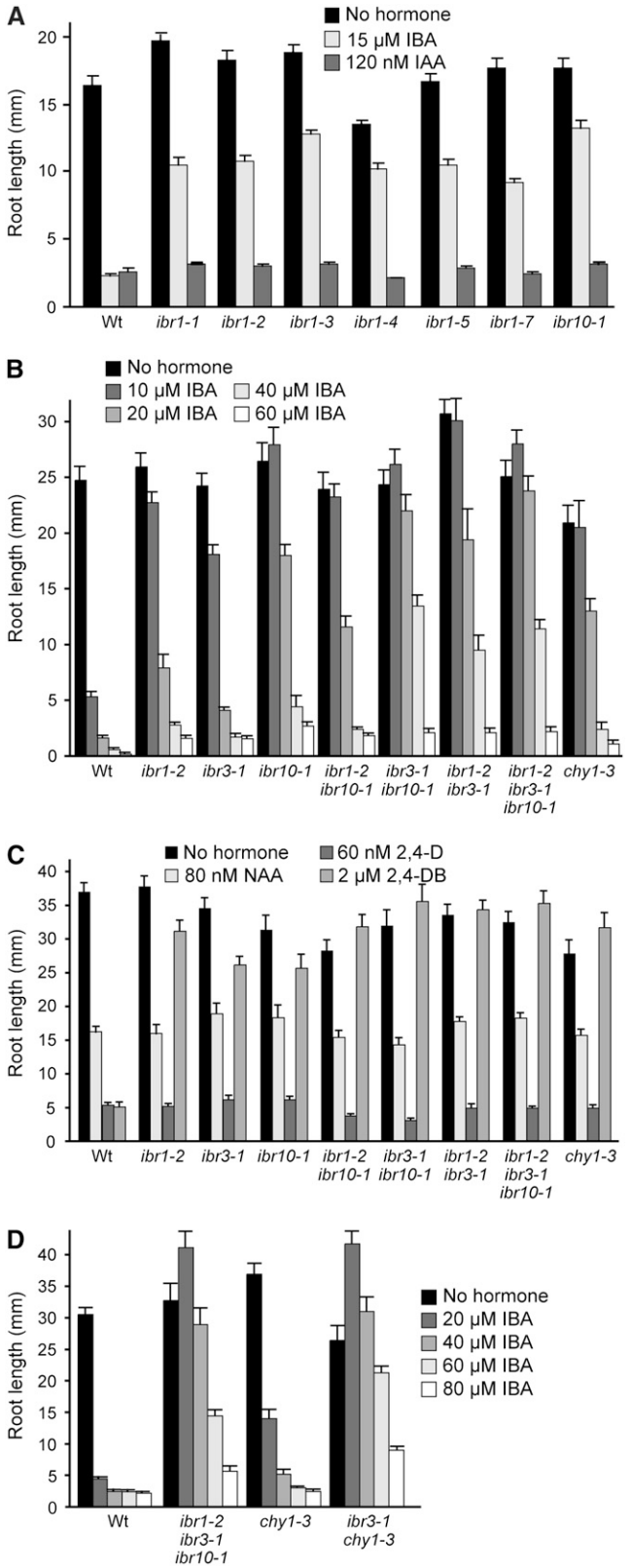

FIGURE 1.—*ibr1* and *ibr10* mutants display IBA- and 2,4-DB-resistant root elongation. (A) *ibr* mutant root elongation on IBA and IAA. Col-0 (Wt), *ibr10-1*, and six *ibr1* alleles were plated on medium containing 0.5% sucrose with no hormone, 15 μM IBA or 120 nM IAA. Root length was measured after 7 days. Error bars show standard errors of mean root lengths ($n \geq 13$). (B) *ibr* mutant root elongation in response to increasing IBA concentrations. Seeds were stratified for 3 days at 4° in 0.1% agar prior to incubation under white light for 2 days at 22°. Germinating seeds were transferred to medium containing 0.5% sucrose (no hormone) or supplemented with the indicated concentration of IBA. Roots were measured after 8 additional days of growth under yellow-filtered light. Error bars show standard errors of mean root lengths ($n \geq 10$). *ibr3-1* (ZOLMAN *et al.* 2007) is included for comparison with *ibr10* and *ibr1*. *chy1-3* (ZOLMAN *et al.* 2001a) is included as an IBA-resistant control. (C) *ibr* mutant root elongation on synthetic auxins. Roots were measured as in B. Error bars show the standard errors of mean root lengths ($n \geq 12$). *chy1-3* is included as a 2,4-DB-resistant control. (D) The *ibr1 ibr3 ibr10* triple mutant remains more IBA responsive than the *ibr3 chy1* double mutant. Root elongation was evaluated as in B. Error bars show standard errors of mean root lengths ($n \geq 8$).

Although the mutants had longer roots than wild type on intermediate IBA levels, all of the mutants responded to IBA at higher concentrations (Figure 1B). We found that *ibr1* was more IBA resistant than *ibr3* and that *ibr10* was more IBA resistant than *ibr1*, *ibr3*, and *chy1* (Figure 1B). Like *ibr3* and *chy1*, *ibr1* and *ibr10* mutants responded normally to IAA (Figure 1A) and to synthetic auxins that are not β-oxidation substrates, such as 1-naphthaleneacetic acid (NAA) and 2,4-D (Figure 1C). *ibr1* and *ibr10* mutants also were resistant to 2,4-DB (Figure 1C), a chain-elongated version of 2,4-D that may be converted to 2,4-D by β-oxidation (HAYASHI *et al.* 1998). The phenotypes of *ibr1* and *ibr10*—resistance to IBA and 2,4-DB coupled with sensitivity to IAA, NAA, and 2,4-D—closely matches the *ibr3* and *chy1* phenotypes.

In addition to assaying root elongation inhibition, we tested the *ibr1* and *ibr10* mutant responses to the stimulatory effects of exogenous auxins on lateral root proliferation. At the concentrations used in our assay, wild-type plants produced similar numbers of lateral roots in response to IBA or NAA induction. Although the *ibr1* and *ibr10* mutants produced normal numbers of lateral roots in response to NAA (Figure 2A) or IAA (data not shown) treatment, both mutants made dramatically fewer lateral roots than wild type in response to IBA stimulation (Figure 2A).

The auxin-inducible DR5-GUS reporter (GUILFOYLE 1999) is expressed in root tips and lateral root primordia, facilitating the visualization of lateral root induction. In wild-type lines carrying the DR5-GUS transgene, lateral root primordia were apparent in response to IBA induction (Figure 2B). In *ibr10-1* DR5-GUS, we found fewer lateral roots and less root staining in response to IBA (Figure 2B). In contrast, we found similar GUS induction throughout *ibr10-1* and wild-type DR5-GUS lines following NAA treatment (Figure 2B). Similar results were seen in *ibr1-2* and *ibr3-1* lines carrying the reporter (data not shown). We concluded from these experiments that, like *ibr3*, *ibr1* and *ibr10* display de-

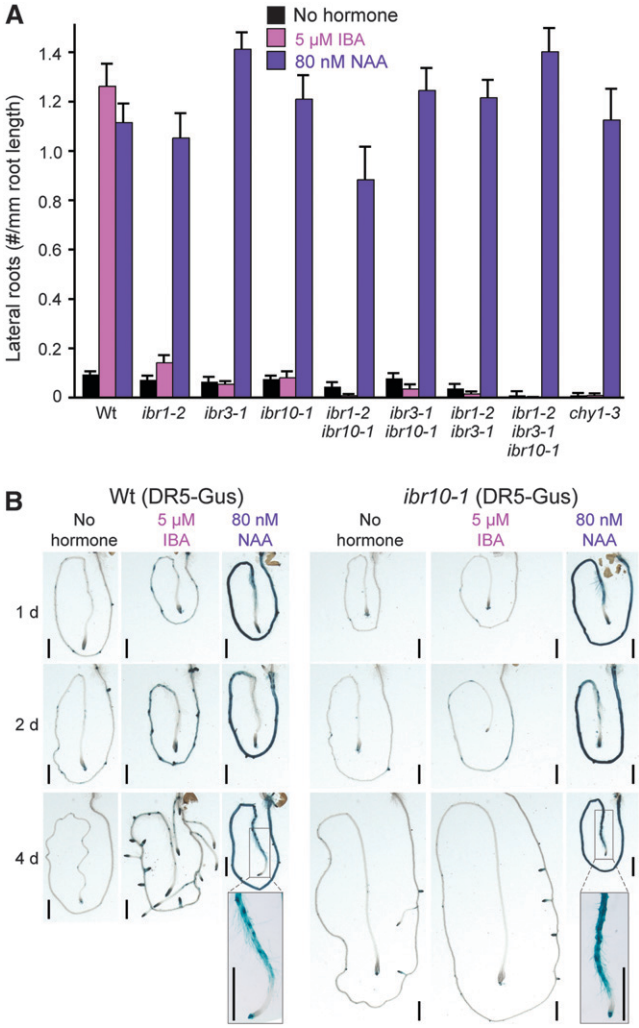

FIGURE 2.—*ibr1* and *ibr10* mutants fail to induce lateral roots in response to IBA. (A) *ibr* mutant lateral root initiation. Seeds were stratified for 3 days at 4° in 0.1% agar prior to plating on medium containing 0.5% sucrose and incubating under white light for 4 days at 22°. Seedlings then were transferred to medium containing 0.5% sucrose with no hormone or supplemented with the indicated concentration of auxin. Roots were measured and lateral roots were counted after 4 additional days of growth. Data are presented as the mean number of lateral roots per millimeter of root length and error bars show the standard error of the means ($n \geq 8$). *chy1-3* is included as an IBA-resistant control. (B) Visualization of *ibr10* lateral root initiation defects using the DR5-GUS reporter. Wild type or *ibr10* containing the DR5-GUS transgene were germinated on medium containing 0.5% sucrose and grown for 4 days and then transferred to unsupplemented medium or medium containing IBA or NAA. After the indicated number of days, seedlings were removed from the medium, stained, and mounted for photography. Lateral root primordia of NAA-treated plants can be visualized in the higher magnification insets. Bars, 1 mm.

fective responses to IBA and 2,4-DB, but maintain normal responses to other auxins.

Higher-order mutants show similar IBA-response phenotypes: Because *ibr1*, *ibr3*, and *ibr10* mutants were all incompletely defective in IBA responses (Figure 1B), we generated double and triple mutants to determine if we could further block IBA responsiveness. In root elongation assays, all of the mutant combinations were IBA resistant compared to wild type at intermediate IBA concentrations (Figure 1B). At very high IBA concentrations, all of the double and triple mutants still responded to IBA. Interestingly, at high IBA concentrations, the *ibr1 ibr3 ibr10* triple mutant was less resistant than the previously described (ZOLMAN *et al.* 2007) *ibr3 chy1* double mutant (Figure 1D). The limited enhancement of IBA resistance seen in higher-order *ibr* mutants suggests that the IBR enzymes may act in the same pathway. The stronger resistance of *ibr3 chy1* suggests that the IBR pathway may promote IBA responses independently of CHY1. *chy1* is believed to indirectly disrupt β-oxidation at the thiolase step (ZOLMAN *et al.* 2001a; LANGE *et al.* 2004).

The double and triple mutants still responded like wild type to NAA and 2,4-D and were 2,4-DB resistant (Figure 1C), consistent with the defect specific to chain-elongated auxins seen in the single *ibr* mutants. Also like the single mutants, the double and triple mutants made few lateral roots in response to IBA induction, but responded like wild type to induction by NAA (Figure 2A). Because so few lateral roots were made in the single mutants in the presence of IBA, we did not attempt to assess the significance of additive or altered effects on lateral rooting in the higher-order mutants.

Other peroxisomal pathways are not detectably disrupted in *ibr1* and *ibr10*: Previously isolated IBA-response mutants fall into two categories: those with general peroxisomal defects, including reduced rates of fatty acid β-oxidation and consequent sucrose dependence during germination, and those that are IBA resistant but appear to carry out other peroxisomal functions normally (ZOLMAN *et al.* 2000). To test whether these new IBA-response alleles had general defects in peroxisomal metabolism manifested in reduced fatty acid β-oxidation, we tested *ibr1* and *ibr10* requirements for sucrose during development. Wild-type seedlings can develop without an exogenous carbon source; early seedling growth is fueled by peroxisomal catabolism of seed storage fatty acids (HAYASHI *et al.* 1998). Mutants defective in seed oil catabolism, due to either loss of a single β-oxidation enzyme or disruption of general peroxisomal function, arrest during early seedling development. Supplementing the growth medium with sucrose, which provides the energy normally obtained from fatty acid β-oxidation, can relieve the arrest. Therefore, comparison of growth with and without exogenous sucrose can reveal defects in peroxisomal function. We found that dark-grown hypocotyls of *ibr1* and *ibr10* elongated normally in the absence of sucrose (Figure 3), suggesting that seed storage fatty acids are efficiently metabolized in both mutants. Indeed, previous gas chromatography–mass spectrometry analysis indicated that seed-storage fatty acids are metabolized

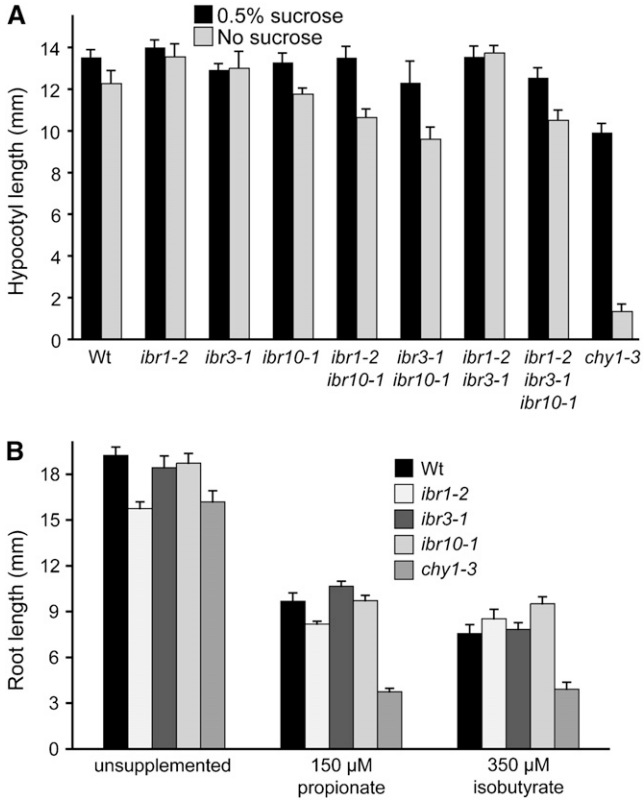

FIGURE 3.—*ibr1* and *ibr10* mutants metabolize peroxisomal substrates similarly to wild type. (A) *ibr* mutant hypocotyl elongation in the absence of sucrose. Seeds were stratified for 4 days at 4° in 0.1% agar prior to plating on unsupplemented medium or medium containing 0.5% sucrose. Plates were placed under white light for 1 day at 22° and then transferred to the dark at 22° for 5 additional days. Error bars show standard errors of mean hypocotyl lengths ($n \geq 10$). *chy1-3* (ZOLMAN *et al.* 2001a) is included as a sucrose-dependent control. (B) *ibr* mutant root elongation on propionate and isobutryate. Seeds were stratified for 3 days at 4° in 0.1% agar prior to incubation under white light for 2 days at 22°. Germinating seeds were transferred to medium containing 0.5% sucrose with or without 150 μM propionate or 350 μM isobutyrate. Roots were measured after 7 additional days of growth. Error bars show standard errors of mean root lengths ($n \geq 11$). *chy1-3* is included as a propionate- and isobutyrate-hypersensitive control (LUCAS *et al.* 2007).

normally during early seedling development in *ibr1-1* and *ibr1-2* (ZOLMAN *et al.* 2000). We also assayed the *ibr* double and triple mutants and found that none displayed sucrose-dependent growth compared to the *chy1* sucrose-dependent control (Figure 3A). We concluded that, even in combination, the *ibr1* and *ibr10* mutations do not appreciably disrupt fatty acid utilization during development.

In addition to IBA and fatty acids, peroxisomes are implicated in the metabolism of other substrates. *CHY1* encodes a peroxisomal β-hydroxybutyryl-CoA hydrolase similar to mammalian mitochondrial enzymes acting in valine catabolism (ZOLMAN *et al.* 2001a). *chy1* mutants are sucrose dependent (ZOLMAN *et al.* 2001a), resistant to IBA (ZOLMAN *et al.* 2001a) and 2,4-DB (LANGE *et al.* 2004), and display heightened sensitivity to root elongation inhibition caused by isobutyrate and propionate treatment (LUCAS *et al.* 2007). These defects are thought to result from accumulation of toxic catabolic intermediates in the mutant. To determine whether the IBR1, IBR3, or IBR10 enzymes might be involved in metabolism of propionate or the branched-chain substrate isobutyrate, we assayed responses of the *ibr* mutants to these compounds. Unlike *chy1*, the *ibr* single-mutant roots were able to elongate like wild type on isobutyrate and propionate (Figure 3B), suggesting that the IBR proteins are not needed for metabolism of these compounds.

acx1 acx5 double mutants have decreased male fertility and reduced jasmonate production, suggesting that peroxisomal ACX enzymes are important for chain shortening of jasmonate precursors (SCHILMILLER *et al.* 2007) in addition to fatty acids (ADHAM *et al.* 2005; PINFIELD-WELLS *et al.* 2005). In contrast, the *ibr1 ibr3 ibr10* triple mutant was fully fertile, suggesting that the IBR enzymes are not essential for jasmonate biosynthesis. Soil-grown *ibr1*, *ibr3*, and *ibr10* single, double, and triple mutants also were not notably different than wild type in size, morphology, or pigmentation (data not shown).

Molecular characterization of the *ibr1* mutants: Using positional information, we mapped the *ibr1* mutant defect to a 3-Mb region in the middle of chromosome 4 between the molecular markers F4C21 and mi167 (Figure 4A). Within this region are the chromosome 4 centromere and a large zone of reduced recombination (COPENHAVEN *et al.* 1999), as well as a chromosomal rearrangement between Col-0 and L*er* (FRANSZ *et al.* 2000). We identified a candidate gene (*At4g05530*) within the *ibr1* mapping interval that encodes a protein in the SDR family with a C-terminal peroxisomal-targeting signal; recent proteomic analysis confirmed that the At4g05530 protein is peroxisomal (REUMANN *et al.* 2007). Because of previous connections between IBA response and peroxisomal function (see above), we hypothesized that disruption of this peroxisomal enzyme might cause the *ibr1* phenotypes.

We sequenced *At4g05530* using DNA from the *ibr1-1* mutant and identified a C-to-T mutation at position 126 (where 1 is the A of the initiator ATG), which alters an Arg to a Cys residue (Figure 4B). Figure 5 shows an alignment of similar proteins from different kingdoms; Arg126 is conserved in 25/25 IBR1 homologs. *ibr1-8* has a mutation at position 1090, which converts a Ser residue to Phe. In *ibr1-2*, we found a G-to-A mutation at position 828 that disrupts the 3′-splice junction following the second intron. The mutation changes the absolutely required G in the splice site, presumably destroying the splice site and altering the downstream protein. In *ibr1-3*, we found a 1-bp deletion at position 859, causing a frameshift in the mutant protein. The first 94 amino acids of the mutant ibr1-3 protein are

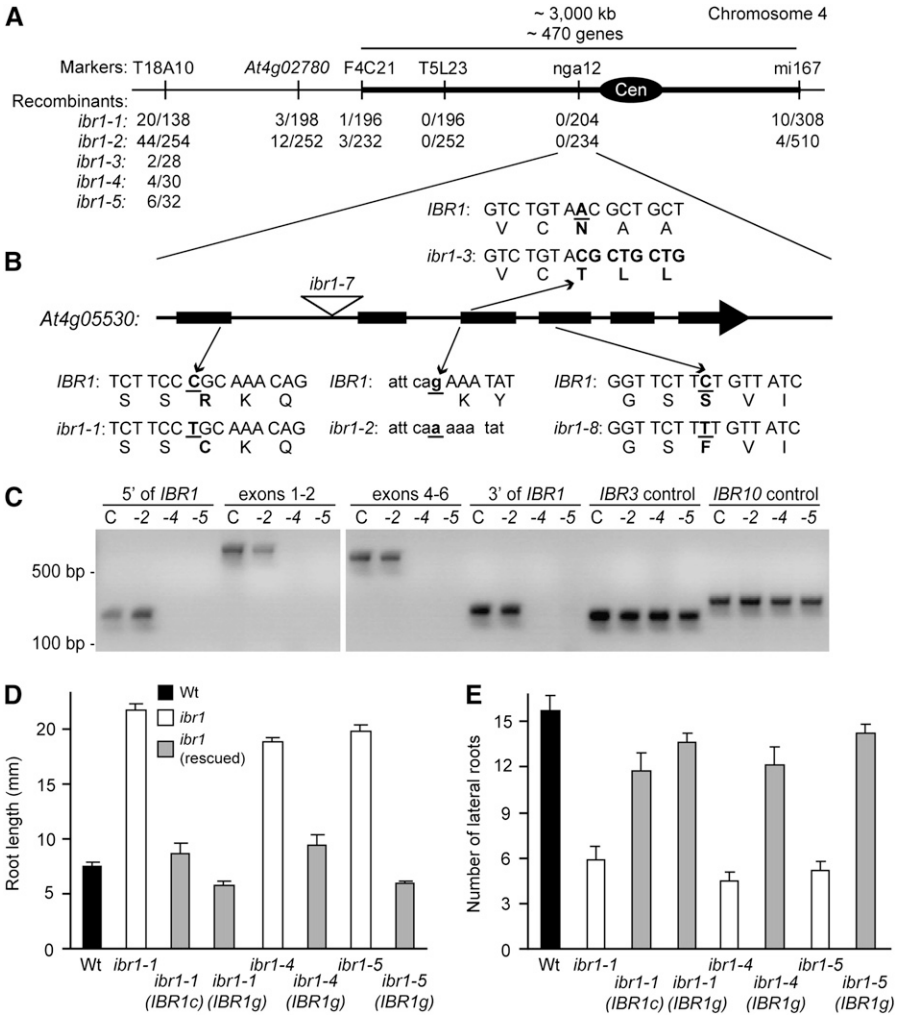

FIGURE 4.—Positional cloning of *IBR1* and complementation of *ibr1* mutants. (A) Recombination mapping of *ibr1* mutant alleles to chromosome 4. IBA-resistant F_2 plants were scored using PCR-based markers (above the bar) and the number of recombination events/total number of chromosomes scored is shown below the bar. The solid oval represents the chromosome 4 centromere. (B) Molecular lesions in *ibr1* mutant alleles. Sequence analysis of the *IBR1* (*At4g05530*) candidate gene (exons shown as solid boxes; introns shown as thin lines) using *ibr1* mutant DNA revealed a C-to-T base-pair change in *ibr1-1*, altering a conserved Arg to Cys. *ibr1-2* has a G-to-A base-pair change at the 3′ splice site of intron 2 (exon sequence is uppercase; intron sequence is lowercase). The *ibr1-3* mutant allele has a 1-bp deletion, leading to a frameshift and premature termination at amino acid 95 (see Figure 5). The position of the *ibr1-7* T-DNA insertion (SALK_010364) is shown by a triangle. *ibr1-8* has a C-to-T base-pair change, altering a Ser residue to Phe. (C) PCR analysis of the *ibr1-4* and *ibr1-5* deletion alleles. Amplification reactions were performed on Col-0 (C), *ibr1-2* (*-2*), *ibr1-4* (*-4*), and *ibr1-5* (*-5*) genomic DNA using primers upstream of *IBR1*, spanning exons 1 and 2, spanning exons 4–6, and downstream of the gene. Control reactions used primers amplifying *IBR3* and *IBR10*. (D) Rescue of *ibr1* defects in IBA-responsive root elongation inhibition by wild-type *IBR1*. Wild-type Col-0 (Wt), *ibr1-1*, *ibr1-4*, and *ibr1-5* mutants and *ibr1* lines containing either 35S-*IBR1c* (*IBR1c*) or pBIN-*IBR1g* (*IBR1g*) were germinated and grown on medium supplemented with 0.5% sucrose and 7.5 μM IBA for 8 days at 22°. Error bars indicate standard errors of the mean root lengths ($n \geq 12$). (E) Rescue of *ibr1* lateral root defects by wild-type *IBR1*. Lines used in D were assayed for lateral root production. Seeds were plated on medium with 0.5% sucrose and grown for 5 days under white light and then transferred to medium further supplemented with 10 μM IBA and grown for 4 additional days. Error bars indicate standard errors of the mean number of visible lateral roots per seedling ($n \geq 12$).

identical to IBR1, followed by 50 amino acids translated in a different frame and a stop codon; the C-terminal peroxisomal-targeting signal in this protein is lost.

The *ibr1-4* and *ibr1-5* mutants were isolated from distinct pools of fast-neutron mutagenized seeds. Both mutants appear to harbor a large deletion removing all of *IBR1*, as multiple primer sets spanning the gene did not amplify products that were present in wild-type samples (Figure 4C). Furthermore, amplification reactions using primers 1500 bp upstream or 850 bp downstream did not yield products. For both *ibr1-4* and *ibr1-5* mutant alleles, we were able to amplify genes in other regions of the genome (Figure 4C), indicating that we had successfully prepared DNA from the mutants. However, we did not explore the precise boundaries of the deletions in either *ibr1-4* or *ibr1-5* and do not know whether additional genes are affected in these alleles.

We obtained a T-DNA insertion mutant (SALK_010364) in *IBR1* from the Salk Institute collection (ALONSO *et al.* 2003). Sequence analysis confirmed that this mutant (*ibr1-7*) had an insertion at position 469 relative to the start codon, near the end of intron 1 (Figure 4B). When we compared the IBA responses of the *ibr1* alleles, we found that all were similarly defective in IBA responsiveness (Figure 1A), indicating that we are likely examining the null phenotype for this gene.

***At4g05530* complements the *ibr1* mutants:** To complement the mutant alleles, we made both a genomic construct driving *IBR1* expression from the *IBR1* 5′ regulatory region and an overexpression construct driving an *IBR1* cDNA from the constitutive 35S promoter from cauliflower mosaic virus. *ibr1-1* was rescued similarly following transformation with either the genomic or overexpression construct (Figure 4, D and E), indicating that both constructs provided sufficient pro-

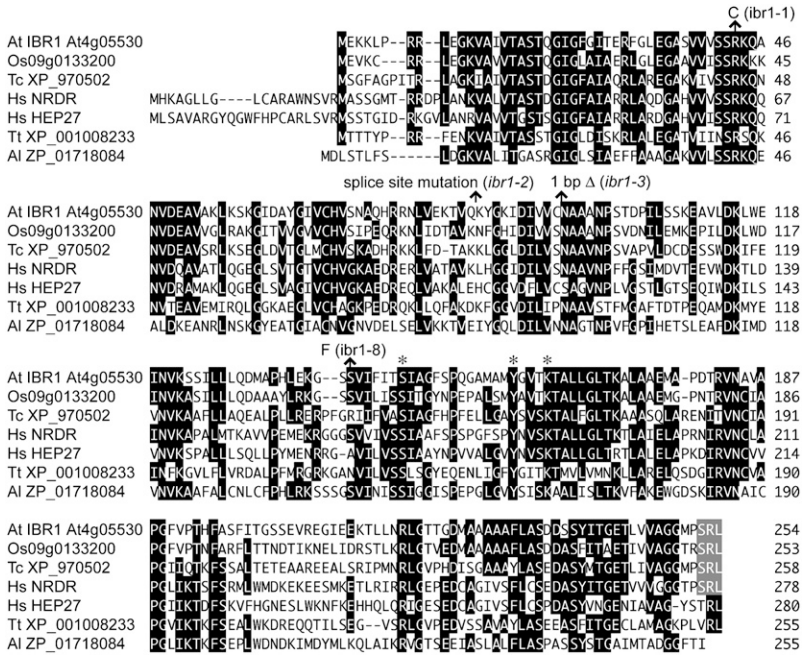

FIGURE 5.—IBR1 resembles short-chain dehydrogenase/reductase enzymes. An alignment comparing IBR1 to similar proteins from rice (Os), beetle (Tc; *Tribolium castaneum*), human (Hs), Tetrahymena (Tt), and the prokaryote *Algoriphagus* sp. PR1 (Al) was generated in the MegAlign program (DNAStar) using the Clustal W method. Amino acid residues identical in at least four sequences are against a solid background; hyphens indicate gaps introduced to maximize alignment. The *ibr1* mutations are indicated above the sequence. The C-terminal PTS1 present in IBR1 and the three closest homologs is indicated by a shaded background; HsHEP27 is not targeted to peroxisomes (PELLEGRINI *et al.* 2002). Asterisks above the sequence denote three essential residues that compose the catalytic triad characteristic of SDR proteins (KALLBERG *et al.* 2002).

tein for wild-type function and that any overexpression did not affect the response. In addition, we found that expression of genomic *IBR1* in *ibr1-3*, *ibr1-4*, and *ibr1-5* restored IBA responses in root elongation and lateral root initiation (Figure 4, D and E, and data not shown). We concluded that the IBA-response defects in *ibr1* result from disruption of the *IBR1/At4g05530* gene.

Molecular characterization of the *ibr10* mutant: We mapped the *ibr10-1* lesion to the middle of chromosome 4, 5.5 Mb below *IBR1* (Figure 6A). Within the mapping region, we identified a gene encoding a putative enoyl-CoA hydratase (*At4g14430*). The At4g14430 protein is similar to enzymes acting in fatty acid β-oxidation (Figure 7) and recently was confirmed to localize in peroxisomes (REUMANN *et al.* 2007). Sequencing this candidate gene revealed a 78-bp deletion in the *ibr10-1* mutant (Figure 6B). This deletion is predicted to remove 26 amino acids from the 240-amino-acid protein, but leave the C terminus in frame with wild-type IBR10. The deletion removes several conserved amino acids; however, a predicted active site residue and the peroxisomal-targeting signal remain in the mutant protein (Figure 7). If the mutant protein is able to fold correctly, retention of this region may be sufficient to allow partial enzyme activity. Because publicly available T-DNA insertion collections contain no insertions in the *At4g14430* coding sequence, we currently are unable to determine whether the single *ibr10-1* allele displays a null phenotype.

***At4g14430* complements the *ibr10-1* mutant:** Because we recovered only a single *ibr10* allele, we sought to confirm that the mutant phenotypes were due to *At4g14430* disruption. We created an *IBR10* overexpression construct that drives expression of *IBR10* from the cauliflower mosaic virus 35S promoter. *ibr10-1* plants transformed with the 35S-*IBR10* construct displayed restored responses to IBA in both root elongation and lateral root initiation assays (Figure 6, C and D), indicating that the identified lesion in *At4g14430* caused the IBA-response defects that we observed in *ibr10-1*.

Mutants defective in the *IBR10* homologs *At4g14440* and *At1g65520* respond normally to IBA: IBR10 has two close Arabidopsis homologs. To determine if either of these proteins contributes to IBA responses, we examined the phenotypes of insertion mutants disrupting these two genes. The closest IBR10 relative in Arabidopsis is At4g14440 (80% identical; Figure 7), which is encoded directly adjacent to *IBR10* and likely results from a recent duplication. However, At4g14440 ends with the C-terminal tripeptide "HNL," which is not a known peroxisomal-targeting signal (REUMANN *et al.* 2004). We isolated a T-DNA insertion line (SALK_012852) predicted to disrupt *At4g14440* (Figure 6B). The mutant responded like wild type to IBA (Figure 6E). We similarly examined a T-DNA insertion allele (SALK_036386) disrupting a second *IBR10* homolog *At1g65520*, which encodes a protein 49% identical to IBR10 that contains the canonical peroxisomal-targeting signal "SKL" (Figure 7). We found that this mutant also displayed wild-type IBA responsiveness (Figure 6E). We concluded that the two closest *IBR10* homologs in the Arabidopsis genome are not required for IBA-responsive root elongation inhibition.

Expression of *IBR* genes: The phenotypic similarities among the *ibr* mutants suggest that IBR1, IBR3, and IBR10 might be involved in similar processes. We used the Genevestigator database of microarray data (ZIMMERMANN *et al.* 2004) to compare the expression

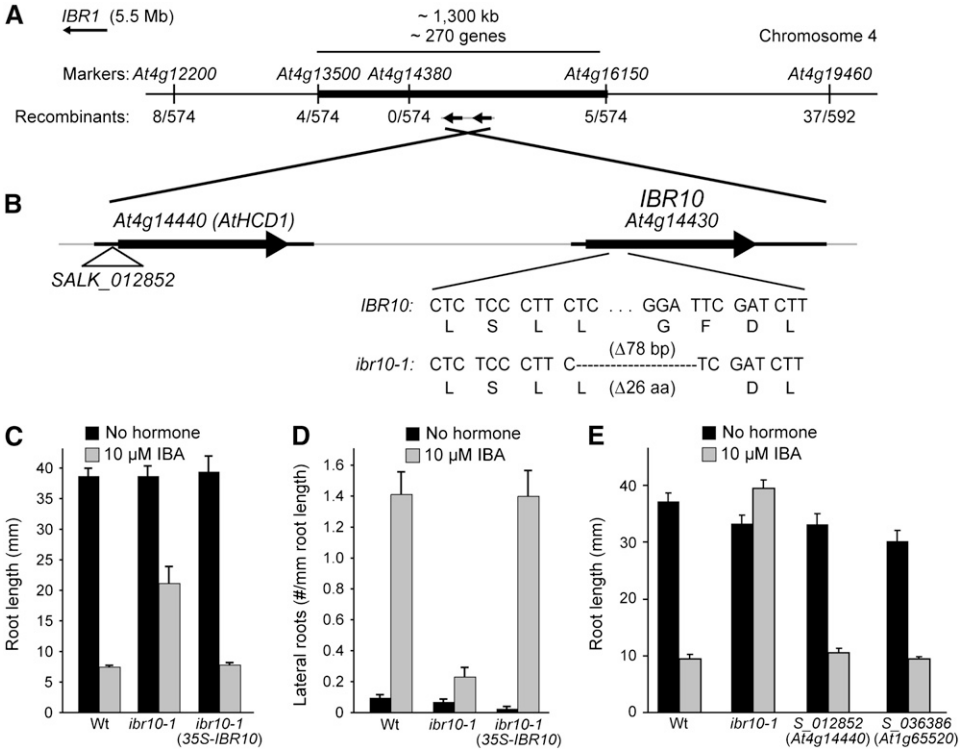

FIGURE 6.—Positional cloning of *IBR10* and complementation of the *ibr10* mutant. (A) Recombination mapping of *ibr10* to the middle of chromosome 4, south of *IBR1*. IBA-resistant F_2 plants were scored using PCR-based markers (above the bar) and the number of recombination events/total number of chromosomes scored is shown below the bar. (B) Molecular lesion in *ibr10-1*. Sequence analysis of the *IBR10* (*At4g14430*) candidate gene using mutant DNA revealed a 78-bp deletion in *ibr10-1*. This deletion removes 26 amino acids of the encoded protein (see Figure 7), but leaves the C terminus of the protein in frame. The position of the T-DNA insertion disrupting the upstream *IBR10* homolog, *AtHCD1/At4g14440*, is indicated by a triangle. (C) Rescue of *ibr10* defects in IBA-responsive root elongation inhibition by wild-type *IBR10*. Wild-type Col-0 (Wt), the *ibr10* mutant, and *ibr10* containing 35S-*IBR10* were assayed as described in the legend for Figure 1B. Error bars show standard errors of mean root lengths ($n \geq 12$). (D) Rescue of *ibr10* lateral root defects by wild-type *IBR10*. Lines used in C were assayed for lateral root production, as described in the legend for Figure 2A. Data are presented as the mean number of lateral roots per millimeter of root length and error bars show the standard error of the means ($n \geq 12$). (E) Root elongation of insertion mutants disrupting *ibr10* homologs. T-DNA insertion mutants in the *ibr10* homologs *AtHCD1/At4g14440* (S_012852) and *ECHIc/At1g65520* (S_036386) were assayed for IBA responses as described in the legend for Figure 1B. Error bars show standard errors of mean root lengths ($n \geq 11$).

patterns of *IBR1*, *IBR3*, and *IBR10* with genes encoding known fatty acid β-oxidation proteins (Figure 8). This analysis revealed that the three *IBR* genes show similar constitutive moderate-level expression in most tissues examined with apparent increases in seeds (Figure 8B). This expression pattern is similar to that of fatty acid β-oxidation genes, except that the fatty acid β-oxidation genes generally have higher expression levels (Figure 8D). In particular, *LACS6*, *LACS7*, *ACX3*, *MFP2*, and *PED1* seem to have a similar pattern as *IBR* gene expression, albeit at apparently higher levels. Interestingly, *IBR1* and *IBR3* transcripts appear to accumulate in senescing leaves, as do many of the fatty acid β-oxidation genes (Figure 8, B and D).

DISCUSSION

The isolation and characterization of two new IBA-response mutants, *ibr1* and *ibr10*, along with the map-based identification of the defective genes, revealed two novel peroxisome-targeted proteins. On the basis of mutant phenotypes and the identity of the encoded proteins, we hypothesize that IBR10 and IBR1 may act in sequential steps in the peroxisomal conversion of IBA to IAA.

IBR10 contains an ECH domain (pfam00378) and has been annotated as ECHIb (REUMANN *et al.* 2007). In a subset of characterized family members, including bacterial hydratases and a yeast isomerase, a conserved Glu residue is required for catalysis (MURSULA *et al.* 2001; WONG and GERLT 2004); this residue is present in IBR10 and retained in the ibr10 mutant protein (Figure 7). The substrates metabolized by ECH enzymes are diverse, although common structural intermediates are typical and there is strong conservation within the CoA-binding site (AGNIHOTRI and LIU 2003). Enzymes in the ECH family often act in reversible reactions and include not only isomerases and hydratases, but also napthoate synthase, carnitine racemase, and hydroxybutyryl-CoA dehydratases. In fatty acid β-oxidation, ECH family enzymes catalyze a hydration reaction to produce hydroxyacyl-CoA thioester intermediates. For example, the Arabidopsis peroxisomal MFP2 and AIM1 multifunctional proteins acting in fatty acid β-oxidation each contain an ECH domain and have enoyl-CoA hydratase activity (RICHMOND and SOMMERVILLE 2000; RYLOTT *et al.* 2006). Unlike these large multifunctional proteins, which also contain L-3-hydroxyacyl-CoA dehydrogenase and D-3-hydroxyacyl-CoA epimerase domains (RICHMOND and SOMMERVILLE 2000; RYLOTT *et al.* 2006), IBR10 is

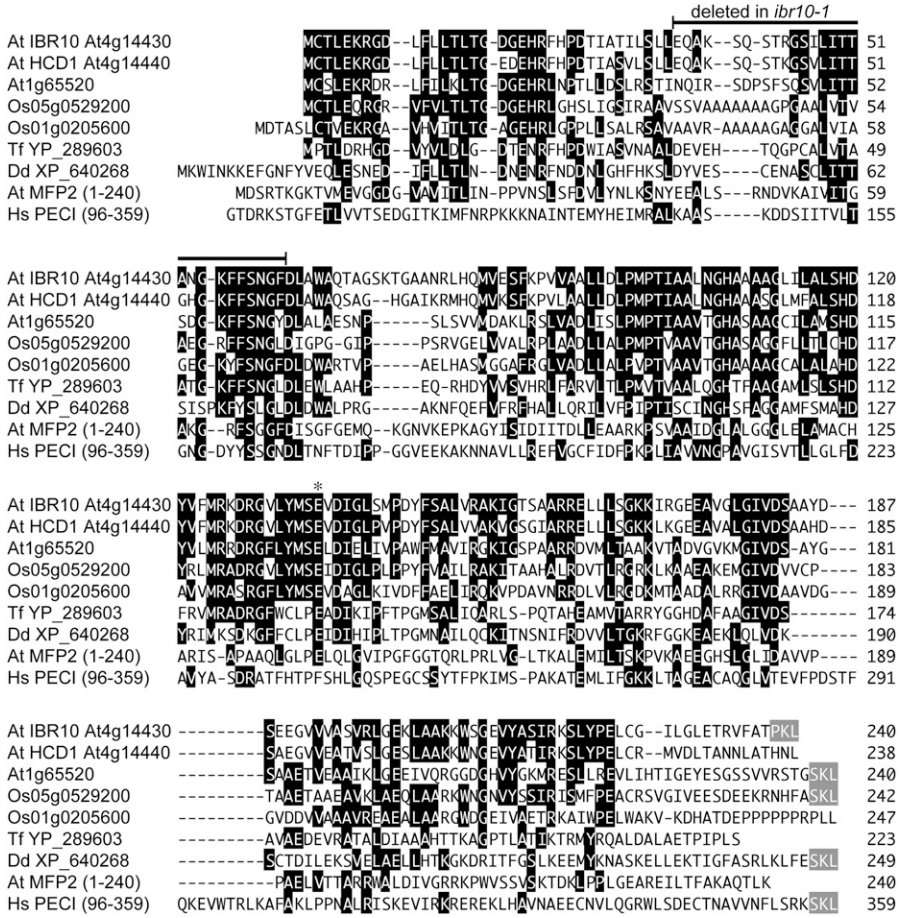

Figure 7.—IBR10 resembles enoyl-CoA hydratases. An alignment comparing IBR10 to similar proteins from Arabidopsis (At), rice (Os), the bacterium *Thermobifida fusca* (Tf), Dictyostelium (Dd), and humans (Hs) was generated in the MegAlign program (DNAStar) using the Clustal W method. Amino acid residues identical in at least four sequences are against a solid background; hyphens indicate gaps introduced to maximize alignment. The *ibr10-1* deletion is indicated above the sequence. The C-terminal PTS1 present in IBR10 and four of the homologs are indicated by a shaded background. The HsPECI homolog has an N-terminal extension compared to the Arabidopsis protein; for clarity, the first 95 amino acids of this protein are not shown. MFP2 is an Arabidopsis multifunctional protein acting in peroxisomal fatty acid β-oxidation that contains enoyl-CoA hydratase/isomerase activity in the first 200 amino acids of the protein (Richmond and Bleecker 1999); the C-terminal domains of MFP2 are not shown. A Glu residue important for activity in a *Pseudomonas putida* hydratase (Wong and Gerlt 2004), a yeast isomerase (Mursula *et al.* 2001), and a rat ECH (Holden *et al.* 2001) is indicated by an asterisk above the sequence.

a single domain protein, reminiscent of enzymes acting in mammalian β-oxidation.

Analysis of other sequenced genomes revealed single-domain IBR10 homologs in several plants, including both monocots and dicots (Reumann *et al.* 2007). The closest IBR10 relative in Arabidopsis is *At4g14440*, which is 80% identical to IBR10 at the amino acid level but lacks a known peroxisomal-targeting signal. This IBR10 homolog, recently named AtHCD1, can act as a *h*ydroxyacyl-*C*o*A* *d*ehydratase on very-long-chain substrates in wax biosynthesis (Garcia *et al.* 2007). An insertion mutant disrupting *AtHCD1* (SALK_012852) contains reduced wax levels and altered wax crystal morphology (Garcia *et al.* 2007). We tested the *hcd1/at4g14440* mutant and found wild-type IBA responses (Figure 6E), suggesting that these two highly related proteins are not functionally redundant in the examined responses. A second Arabidopsis homolog, At1g65520 (ECHIc), is 49% identical to IBR10 and is peroxisomal (Reumann *et al.* 2007); disruption of *At1g65520* also did not alter IBA responses (Figure 6E). Rice contains two clear IBR10 homologs; as in Arabidopsis, one has a predicted peroxisomal localization whereas the other does not (Figure 7).

Outside the plant kingdom, IBR10 has limited similarity (~20% identical) to a mammalian *p*eroxisomal *e*noyl-*C*o*A* *i*somerase (PECI; Geisbrecht *et al.* 1999) that is localized in both peroxisomes and mitochondria (Geisbrecht *et al.* 1999; Zhang *et al.* 2002). This enzyme has $\Delta^3\Delta^2$enoyl-CoA isomerase activity (Geisbrecht *et al.* 1999), which is required for rearranging double bonds to allow complete β-oxidation of unsaturated fatty acids. The *Saccharomyces cerevisiae* homolog, Eci1p, also has isomerase activity but lacks hydratase activity (Geisbrecht *et al.* 1998). Human PECI has an N-terminal extension compared to the other homologs (Figure 7) that resembles acyl-CoA-binding proteins (Poirier *et al.* 2006).

IBR1 is in the SDR family, a large group of proteins with highly variable enzymatic functions. SDR proteins can have oxidoreductase, lyase, isomerase, or related activities and act on a wide variety of substrates, including steroids, sugars, and alcohols. Each enzyme requires NAD, NADP, or FAD as an electron carrier, which typically is bound by a Rossman fold within the N-terminal region of the protein; the identity of this cofactor is used as a partial determinant of enzyme classification (Kallberg *et al.* 2002; Kallberg and Persson 2006). The C-terminal region is typically less conserved and is important for substrate interactions.

Arabidopsis IBR1 is in the dehydrogenase subcategory with different or unknown specificities (FabG/

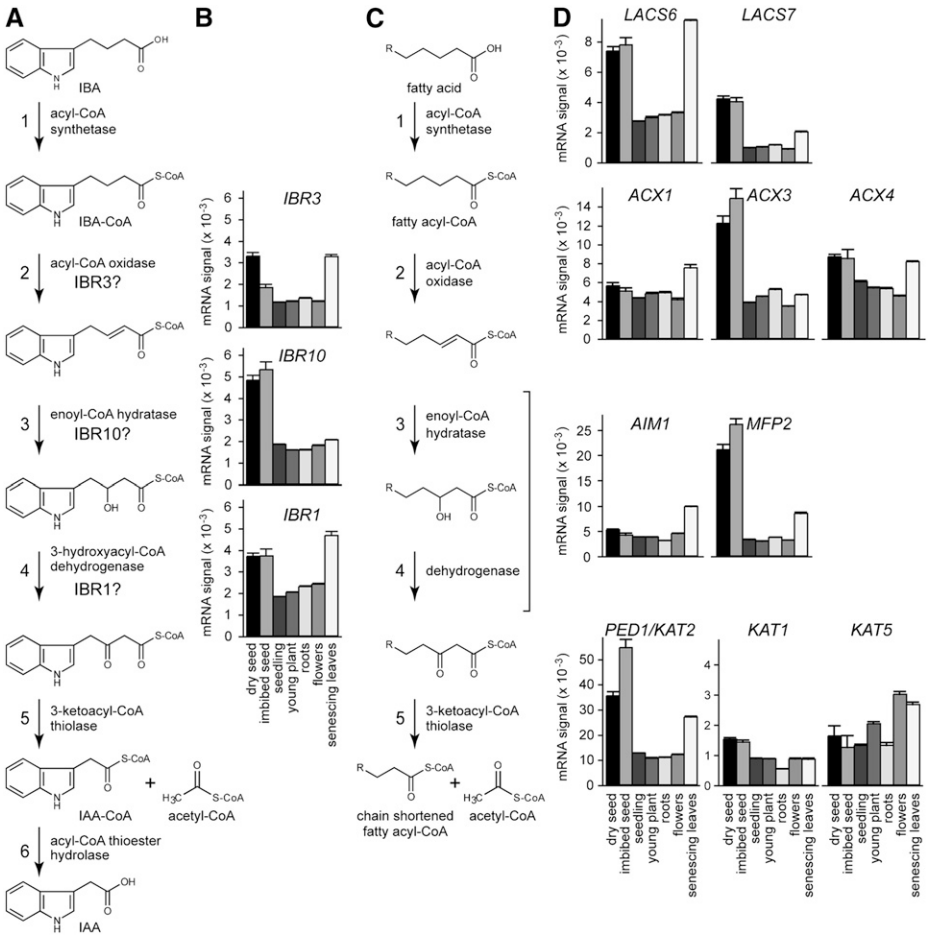

FIGURE 8.—Expression profiles of genes encoding IBR enzymes and enzymes acting in fatty acid β-oxidation. (A) A model for the conversion of IBA to IAA. General enzymatic requirements are shown to the right of the arrows along with the hypothesized positions for IBR3, IBR10, and IBR1 activity. (B) Relative expression levels (mRNA signal) for *IBR3*, *IBR10*, and *IBR1* in several Arabidopsis tissues. Genevestigator (ZIMMERMANN *et al.* 2004) data indicate that expression of the three *IBR* genes is similar among tissues. Error bars show the standard error of the mean expression levels; $n = 121$ for dry seeds, 26 for imbibed seeds, 944 for seedlings, 419 for young plants, 330 for roots, 619 for flowers, and 3 for senescing leaves. Data were retrieved from Genevestigator in June 2008. (C) Pathway of fatty acid β-oxidation, where R represents a side-chain extension of additional carbon units. In plant peroxisomes, step 1 is catalyzed by long-chain acyl-CoA synthetases (LACS6 and LACS7), step 2 is catalyzed by a family of acyl-CoA oxidases (ACX1-6), steps 3 and 4 are catalyzed by multifunctional proteins (AIM1 or MFP2), and step 5 is carried out by thiolase (PED1/KAT2, KAT1, and KAT5). (D) Relative expression levels (mRNA signal) for genes encoding fatty acid β-oxidation enzymes in several Arabidopsis tissues. Genevestigator data were collected as described in B.

COG1028 and COG4221; MARCHLER-BAUER and BRYANT 2004). On the basis of protein size and amino acid residues at conserved domains, IBR1 has been classified as a "classical" SDR (KALLBERG *et al.* 2002, 2007) and also has been annotated as SDRa (REUMANN *et al.* 2007). IBR1 has an apparent nucleotide-binding site with a predicted preference for an NADP(H) cofactor (http://www.ifm.liu.se/bioinfo/; KALLBERG and PERSSON 2006). In addition, the three SDR catalytic amino acids (KALLBERG *et al.* 2002) are conserved in IBR1 (Ser146, Tyr159, and Lys163), along with other less tightly conserved amino acid sequences indicative of SDR classification (Figure 5; KALLBERG *et al.* 2002; REUMANN *et al.* 2007).

IBR1 homologs are present in animals, bacteria, and plants. According to the classification system of KALLBERG *et al.* (2007), IBR1 is the only Arabidopsis family member in cluster 5c. Human HEP27 (also known as DHRS2) is the most characterized member of this cluster and is 45% identical to IBR1. HEP27 is a nuclear protein (PELLEGRINI *et al.* 2002) and can reduce dicarbonyl compounds, but not sugars, steroids, or retinoids (SHAFQAT *et al.* 2006). The mammalian protein NRDR (also known as DHRS4, HEP27-like, RRD, PHCR, SDR-SRL, and SCAD-SRL) is a closely related homolog that acts as a retinol dehydrogenase and a retinal reductase regulating retinoid metabolism (LEI *et al.* 2003). This enzyme has an "SRL" peroxisomal-targeting signal, like Arabidopsis IBR1, and has been shown to localize to peroxisomes using a fluorescent reporter protein (FRANSEN *et al.* 1999). Furthermore, NRDR activity has been isolated from mouse peroxisomes and increases in the presence of peroxisome proliferators (LEI *et al.* 2003). Although characterization of the human NRDR protein lends credence to the importance of IBR1 in peroxisomal metabolic pathways, retinol (vitamin A) or retinal are unlikely substrates for IBR1, as these molecules are not observed in plants (WOLF 1984).

Recent proteomic analysis of soybean peroxisomal proteins revealed GmSDR, which is 78% identical to IBR1 (ARAI *et al.* 2008), and analysis of sequenced databases identified IBR1 homologs in a variety of monocot and dicot species (REUMANN *et al.* 2007). None of the closely related IBR1 plant homologs have known substrates, although a *Solanum tuberosum* tropinone reductase (34% identical to IBR1) has been characterized (KEINER *et al.* 2002). Tropinone reduc-

tases are NADPH-dependent enzymes acting in alkaloid metabolism; these enzymes do not appear to be localized to peroxisomes. More distant Arabidopsis relatives include ABA2, which acts in ABA biosynthesis (Cheng *et al.* 2002), and the ATA1 enzyme homologous to TASSELSEED 2 (Lebel-Hardenack *et al.* 1997), involved in sex determination in maize (Delong *et al.* 1993).

We can envision both direct and indirect mechanisms by which defects in peroxisomal enzymes might reduce IBA responsiveness. In the direct model, IBR enzymes would catalyze IBA β-oxidation reactions. The specificity of the *ibr* defects and the nature of the mutated genes are consistent with the possibility that IBR1 and IBR10 act directly in the conversion of IBA to IAA (Figure 8A). Because elimination of two carbons could convert IBA to IAA, we expect that the responsible enzymes will resemble those acting in fatty acid β-oxidation. In plants, fatty acid β-oxidation occurs by addition of a CoA moiety by an acyl-CoA synthetase followed by the repeating activities of ACX, MFP, and thiolase enzymes (Figure 8C). Previously, we suggested that IBR3 might act as an IBA-CoA dehydrogenase or oxidase, carrying out the second step in IBA β-oxidation (Figure 8A, step 2; Zolman *et al.* 2007). The multifunctional proteins AIM1 (Richmond and Bleecker 1999) and MFP2 (Rylott *et al.* 2006) are isozymes with different chain-length specificities that carry out steps 3 and 4 of fatty acid β-oxidation, which involve a hydration and subsequent NAD^+-dependent dehydrogenation. AIM1 also might act in the conversion of IBA, as the *aim1* mutant is resistant to IBA (Zolman *et al.* 2000) and 2,4-DB (Richmond and Bleecker 1999). However, identification of *IBR10*, which encodes an enoyl-CoA hydratase/isomerase family member, and *IBR1*, which encodes a dehydrogenase/reductase-like protein, suggests that IBR10 and IBR1 may together provide AIM1 activity in IBA β-oxidation, either in addition to or instead of AIM1.

The activities of biochemically characterized enzymes similar to IBR1 and IBR10 fit with what would be required for IBA β-oxidation. *ibr1* and *ibr10*, along with *ibr3* (Zolman *et al.* 2007), have specific defects in IBA responses, displaying reduced responses to IBA in root elongation, lateral root initiation assays, and IBA-induced reporter gene expression, but normal responses to other forms of auxin (Figures 1 and 2). Because neither *ibr1* nor *ibr10* have phenotypes typical of fatty acid β-oxidation defects (sucrose dependence during early development; Figure 3A), the disruptions of these genes are unlikely to affect general peroxisomal function or fatty acid β-oxidation. Genetic evidence suggests that IBA-to-IAA conversion is peroxisomal; therefore, we expect enzymes catalyzing this conversion to be peroxisomally targeted. Both IBR1 ("SRL") and IBR10 ("PKL") have predicted C-terminal type 1 peroxisomal-targeting signals (Kamada *et al.* 2003; Reumann *et al.* 2004) and recent proteomic analysis of purified peroxisomes and YFP-localization studies confirm that both IBR1 and IBR10 are peroxisomal (Reumann *et al.* 2007), consistent with a role in IBA metabolism.

Rather than directly catalyzing IBA β-oxidation, IBR1 and IBR10 might act in other peroxisomal processes that, when disrupted, indirectly impede IBA metabolism. An indirect model for IBA β-oxidation disruption is not without precedent. Such a mechanism might result from accumulation of toxic intermediates, as in the *chy1* mutant (Zolman *et al.* 2001a). CHY1 encodes a β-hydroxyisobutyryl-CoA hydrolase acting in peroxisomal valine (Zolman *et al.* 2001a; Lange *et al.* 2004) or isobutyrate (Lucas *et al.* 2007) catabolism. *chy1* mutants are sucrose dependent (Zolman *et al.* 2001a), IBA resistant (Zolman *et al.* 2001a), 2,4-DB resistant (Lange *et al.* 2004), and hypersensitive to isobutyrate and propionate (Lucas *et al.* 2007). These phenotypes are thought to result from accumulation of a toxic valine catabolic intermediate that impedes thiolase activity (Zolman *et al.* 2001a; Lange *et al.* 2004). The *ibr1*, *ibr3*, and *ibr10* mutants respond like wild type to exogenous isobutyrate and propionate (Figure 3B), suggesting that the IBR proteins do not act in the CHY1 pathway.

A second potential indirect mechanism for disruption of IBA β-oxidation is decreased cofactor availability. For example, disrupting the second step of fatty acid β-oxidation (Figure 8) in certain *acx* mutants leads to accumulation of fatty acyl-CoA esters (Rylott *et al.* 2003; Pinfield-Wells *et al.* 2005). These activated, but unprocessed, substrates might deplete the CoA pool available to IBA and thereby limit IBA metabolism to IAA (Adham *et al.* 2005).

If IBR1 acts directly in IBA β-oxidation, it is curious that the protein is in the short-chain alcohol dehydrogenase/reductase family rather than resembling acyl-CoA dehydrogenases, as might be expected for an enzyme acting at this step of the pathway. However, the SDR family has a broad list of accepted substrates, perhaps indicating a catalytic pocket that could accommodate the IBA β-oxidation intermediate. Previous bioinformatic analysis led to the suggestion that IBR1 might act on β-hydroxyisobutyrate (Reumann *et al.* 2004); this model is attractive because the potential substrate lacks a CoA side chain. However, it is unclear how a block this late in valine catabolism would impede IBA responsiveness. Unlike the *chy1* mutant that is disrupted in valine catabolism, *ibr1* mutants are not sucrose dependent (Figure 3A). Moreover, in contrast to *chy1*, *ibr1* does not display increased sensitivity to isobutyrate or propionate (Figure 3B).

Ultimately, testing these competing hypotheses will require biochemical assays to determine the preferred substrates and specific activity of each enzyme. If potential substrates become available, we will be able to determine the nature of the activity of the IBR enzymes on intermediates in IBA metabolism, revealing each as a direct enzymatic player or as an indirect

participant acting in a pathway that overlaps or interferes with IBA metabolism in the peroxisome. In addition to determining the enzymatic activity of IBR1, IBR3, and IBR10, enzymes catalyzing other steps of the pathway remain to be identified. The activating enzyme that adds CoA onto IBA (Figure 8, step 1) has not been identified; LACS6 and LACS7 act on fatty acid substrates but appear not to act on IBA (Fulda *et al.* 2004). In addition, the enzyme acting in the thiolase step (Figure 8, step 5) has not been established. Although PED1 is the best-characterized and most active thiolase, two other thiolases (KAT1 and KAT5) are encoded in the Arabidopsis genome (Germain *et al.* 2001; Carrie *et al.* 2007) and could act on IBA intermediates. Furthermore, we expect that an enzyme to remove the CoA moiety (Figure 8, step 6) will be required; several thioesterases with unknown substrates are predicted to reside in the peroxisome (Reumann *et al.* 2004) and may catalyze this reaction. Finally, IAA acts outside of the peroxisome and therefore a transporter is expected to export the active auxin; whether this transporter removes IAA or IAA-CoA also is an open question.

Although our genetic evidence in Arabidopsis suggests that IBA must be converted to IAA to exert auxin activity, IBA is proposed to promote lateral root formation in rice independently of IAA signaling (Chhun *et al.* 2003). Interestingly, IBR3 (Zolman *et al.* 2007), IBR1 (Figure 5), and IBR10 (Figure 7) all have close homologs in rice that are predicted to be peroxisomal; the conservation of these proteins hints that IBA β-oxidation may play a role in auxin metabolism in rice as well. Further examination of these proteins and IBA metabolism in a variety of plants will reveal whether different species have evolved different roles for IBA in auxin metabolism and action.

Appropriate production, transport, and storage of IAA are essential for normal plant development. Our genetic studies implicate the peroxisomal enzymes IBR1 and IBR10 as likely players in the β-oxidation of IBA to free IAA, in conjunction with the previously characterized IBR3. Continued elucidation of the regulation and mechanism of this conversion will provide a more complete understanding of inputs into the auxin pool and the control of auxin homeostasis.

We thank the Arabidopsis Biological Resource Center at Ohio State University for seeds and DNA stocks; the Salk Institute Genomic Analysis Laboratory for generating the sequence-indexed Arabidopsis T-DNA insertion mutants; and Matthew Lingard, Sarah Ratzel, Lucia Strader, and Andrew Woodward for critical comments on the manuscript. This research was supported by the University of Missouri at St. Louis start-up funds, the University of Missouri Research Board, the National Science Foundation (NSF) (IBN-0315596 and MCB-0745122), and the Robert A. Welch Foundation (C-1309). N.M. was supported in part by the Rice-Houston Alliance for Graduate Education and the Professoriate program (NSF HRD-0450363) and the National Institutes of Health (NIH) (F31-GM081911), A.M. was supported in part by an American Society of Plant Biologists' Summer Undergraduate Research Fellowship, and A.R.A. was supported by the NIH (F31-GM066373) and a Houston Livestock Show and Rodeo Fellowship.

LITERATURE CITED

Adham, A. R., B. K. Zolman, A. Millius and B. Bartel, 2005 Mutations in Arabidopsis acyl-CoA oxidase genes reveal distinct and overlapping roles in β-oxidation. Plant J. **41:** 859–874.

Agnihotri, G., and H.-W. Liu, 2003 Enoyl-CoA hydratase: reaction, mechanism, and inhibition. Bioorg. Med. Chem. **11:** 9–20.

Alonso, J. M., A. N. Stepanova, T. J. Leisse, C. J. Kim, H. Chen *et al.*, 2003 Genome-wide insertional mutagenesis of *Arabidopsis thaliana.* Science **301:** 653–657.

Arai, Y., M. Hayashi and M. Nishimura, 2008 Proteomic analysis of highly purified peroxisomes from etiolated soybean cotyledons. Plant Cell Physiol. **49:** 526–539.

Ausubel, F. M., R. Brent, R. E. Kingston, D. D. Moore, J. G. Seidman *et al.*, 1999 *Current Protocols in Molecular Biology.* Greene Publishing Associates and Wiley-Interscience, New York.

Baker, A., I. Graham, M. Holdsworth, S. Smith and F. Theodoulou, 2006 Chewing the fat: beta-oxidation in signalling and development. Trends Plant Sci. **11:** 124–132.

Bartel, B., and G. R. Fink, 1994 Differential regulation of an auxin-producing nitrilase gene family in *Arabidopsis thaliana.* Proc. Natl. Acad. Sci. USA **91:** 6649–6653.

Bartel, B., and G. R. Fink, 1995 ILR1, an amidohydrolase that releases active indole-3-acetic acid from conjugates. Science **268:** 1745–1748.

Bartel, B., S. LeClere, M. Magidin and B. K. Zolman, 2001 Inputs to the active indole-3-acetic acid pool: *de novo* synthesis, conjugate hydrolysis, and indole-3-butyric acid β-oxidation. J. Plant Growth Regul. **20:** 198–216.

Bennett, M. J., A. Marchant, H. G. Green, S. T. May, S. P. Ward *et al.*, 1996 *Arabidopsis AUX1* gene: a permease-like regulator of root gravitropism. Science **273:** 948–950.

Bevan, M., 1984 Binary *Agrobacterium* vectors for plant transformation. Nucleic Acids Res. **12:** 8711–8721.

Carrie, C., M. W. Murcha, A. H. Millar, S. M. Smith and J. Whelan, 2007 Nine 3-ketoacyl-CoA thiolases (KATs) and acetoacetyl-CoA thiolases (ACATs) encoded by five genes in Arabidopsis thaliana are targeted either to peroxisomes or cytosol but not to mitochondria. Plant Mol. Biol. **63:** 97–108.

Cheng, W.-H., A. Endo, L. Zhou, J. Penney, H.-C. Chen *et al.*, 2002 A unique short-chain dehydrogenase/reductase in Arabidopsis glucose signaling and abscisic acid biosynthesis and functions. Plant Cell **14:** 2723–2743.

Chhun, T., S. Taketa, S. Tsurumi and M. Ichii, 2003 The effects of auxin on lateral root initiation and root gravitropism in a lateral rootless mutant *Lrt1* of rice (*Oryza sativa L.*). Plant Growth Regul. **39:** 161–170.

Clough, S. J., and A. F. Bent, 1998 Floral dip: a simplified method for *Agrobacterium*-mediated transformation of *Arabidopsis thaliana.* Plant J. **16:** 735–743.

Copenhaven, G. P., K. Nickel, T. Kuromori, M. Benito, S. Kaul *et al.*, 1999 Genetic definition and sequence analysis of *Arabidopsis* centromeres. Science **286:** 2468–2474.

Davies, R. T., D. H. Goetz, J. Lasswell, M. N. Anderson and B. Bartel, 1999 *IAR3* encodes an auxin conjugate hydrolase from Arabidopsis. Plant Cell **11:** 365–376.

DeLong, A., A. Calderon-Urrea and S. L. Dellaporta, 1993 Sex determination gene TASSELSEED2 of maize encodes a short-chain alcohol dehydrogenase required for stage-specific floral organ abortion. Cell **74:** 757–768.

Eastmond, P. J., and I. A. Graham, 2000 The multifunctional protein AtMFP2 is co-ordinately expressed with other genes of fatty acid β-oxidation during seed germination in *Arabidopsis thaliana* (L.). Heynh. Biochem. Soc. Trans. **28:** 95–99.

Eastmond, P. J., V. Germain, P. R. Lange, J. H. Bryce, S. M. Smith *et al.*, 2000 Postgerminative growth and lipid catabolism in oilseeds lacking the glyoxylate cycle. Proc. Natl. Acad. Sci. USA **97:** 5669–5674.

Fan, J., S. Quan, T. Orth, C. Awai, J. Chory *et al.*, 2005 The Arabidopsis PEX12 gene is required for peroxisome biogenesis and is essential for development. Plant Physiol. **139:** 231–239.

Fawcett, C. H., R. L. Wain and F. Wightman, 1960 The metabolism of 3-indolylalkanecarboxylic acids, and their amides, nitriles and methyl esters in plant tissues. Proc. R. Soc. Lond. Ser. B **152:** 231–254.

Footitt, S., S. P. Slocombe, V. Larner, S. Kurup, Y. Wu *et al.*, 2002 Control of germination and lipid mobilization by *COMATOSE*, the *Arabidopsis* homologue of human ALDP. EMBO J. **21:** 2912–2922.

Fransen, M., P. Van Veldhoven and S. Subramani, 1999 Identification of peroxisomal proteins by using M13 phage protein VI phage display: molecular evidence that mammalian peroxisomes contain a 2,4-dienoyl-CoA reductase. Biochem. J. **340:** 561–568.

Fransz, P. F., S. Armstrong, J. H. de Jong, L. D. Parnell, C. van Drunen *et al.*, 2000 Integrated cytogenic map of chromosome arm 4S of *A. thaliana*: structural organization of of heterochromatic knob and centromere region. Cell **100:** 367–376.

Froman, B. E., P. C. Edwards, A. G. Bursch and K. Dehesh, 2000 ACX3, a novel medium-chain acyl-coenzyme A oxidase from Arabidopsis. Plant Physiol. **123:** 733–741.

Fulda, M., J. Schnurr, A. Abbadi, E. Heinz and J. Browse, 2004 Peroxisomal acyl-CoA synthetase activity is essential for seedling development in *Arabidopsis thaliana*. Plant Cell **16:** 394–405.

Fulda, M., J. Shockey, M. Werber, F. P. Wolter and E. Heinz, 2002 Two long-chain acyl-CoA synthetases from *Arabidopsis thaliana* involved in peroxisomal fatty acid β-oxidation. Plant J. **32:** 93–103.

Garcia, C., J. Joubes, S. Chevalier, J. Laroche-Traineau, B. Bourdenx *et al.*, 2007 *AtHCD1* encodes a 3-hydroxyacyl-CoA dehydratase involved in wax biosynthesis in *Arabidopsis thaliana*, pp. 203–206 in *17th International Symposium on Plant Lipids*, edited by C. Benning and J. Ohlrogge. Aardvark Global, East Lansing, MI.

Geisbrecht, B. V., D. Zhu, K. Schultz, K. Nau, J. C. Morrell *et al.*, 1998 Molecular characterization of *Saccharomyces cerevisiae* delta3, delta2-enoyl-CoA isomerase. J. Biol. Chem. **273:** 33184–33191.

Geisbrecht, B. V., D. Zhang, H. Schulz and S. J. Gould, 1999 Characterization of PECI, a novel monofunctional delta 3,delta 2-enoyl-CoA isomerase of mammalian peroxisomes. J. Biol. Chem. **274:** 21797–21803.

Germain, V., E. L. Rylott, T. R. Larson, S. M. Sherson, N. Bechntold *et al.*, 2001 Requirement for 3-ketoacyl-CoA thiolase-2 in peroxisome development, fatty acid β-oxidation and breakdown of triacylglycerol in lipid bodies of *Arabidopsis* seedlings. Plant J. **28:** 1–12.

Graham, I. A., and P. J. Eastmond, 2002 Pathways of straight and branched chain fatty acid catabolism in higher plants. Prog. Lipid Res. **41:** 156–181.

Guilfoyle, T. J., 1999 Auxin-regulated genes and promoters, pp. 423–459 in *Biochemistry and Molecular Biology of Plant Hormones*, edited by P. J. J. Hooykaas, M. A. Hall and K. R. Libbenga. Elsevier, Amsterdam.

Haughn, G. W., and C. Somerville, 1986 Sulfonylurea-resistant mutants of *Arabidopsis thaliana*. Mol. Gen. Genet. **204:** 430–434.

Hayashi, H., L. De Bellis, A. Ciurli, M. Kondo, M. Hayashi *et al.*, 1999 A novel acyl-CoA oxidase that can oxidize short-chain acyl-CoA in plant peroxisomes. J. Biol. Chem. **274:** 12715–12721.

Hayashi, H., K. Nito, R. Takei-Hoshi, M. Yagi, M. Kondo *et al.*, 2002 Ped3p is a peroxisomal ATP-binding cassette transporter that might supply substrates for fatty acid β-oxidation. Plant Cell Physiol. **43:** 1–11.

Hayashi, M., K. Toriyama, M. Kondo and M. Nishimura, 1998 2,4-Dichlorophenoxybutyric acid-resistant mutants of Arabidopsis have defects in glyoxysomal fatty acid β-oxidation. Plant Cell **10:** 183–195.

Holden, H. M., M. M. Benning, T. Haller and J. A. Gerlt, 2001 The crotonase superfamily: divergently related enzymes that catalyze different reactions involving acyl coenzyme A thioesters. Acc. Chem. Res. **34:** 145–157.

Hooks, M. A., F. Kellas and I. A. Graham, 1999 Long-chain acyl-CoA oxidases of *Arabidopsis*. Plant J. **20:** 1–13.

Kallberg, Y., and B. Persson, 2006 Prediction of coenzyme specificity in dehydrogenases/reductases. FEBS J. **273:** 1177–1184.

Kallberg, Y., U. Oppermann, H. Jornvall and B. Persson, 2002 Short-chain dehydrogenase/reductases (SDRs): coenzyme-based functional assignments in completed genomes. Eur. J. Biochem. **269:** 4409–4417.

Kallberg, Y., U. Oppermann, H. Jornvall and B. Persson, 2007 Short-chain dehydrogenase/reductase (SDR) relationships: a large family with eight clusters common to human, animal, and plant genomes. Protein Sci. **11:** 636–641.

Kamada, T., K. Nito, H. Hayashi, S. Mano, M. Hayashi *et al.*, 2003 Functional differentiation of peroxisomes revealed by expression profiles of peroxisomal genes in *Arabidopsis thaliana*. Plant Cell Physiol. **44:** 1275–1289.

Keiner, R., H. Kaiser, K. Nakajima, T. Hashimoto and B. Drager, 2002 Molecular cloning, expression and characterization of tropinone reductase II, an enzyme of the SDR family in Solanum tuberosum (L.). Plant Mol. Biol. **48:** 299–308.

Koncz, C., J. Schell and G. P. Rédei, 1992 T-DNA transformation and insertion mutagenesis, pp. 224–273 in *Methods in Arabidopsis Research*, edited by C. Koncz, N.-H. Chua and J. Schell. World Scientific, Singapore.

Lange, P., P. Eastmond, K. Madagan and I. Graham, 2004 An Arabidopsis mutant disrupted in valine catabolism is also compromised in peroxisomal fatty acid beta-oxidation. FEBS Lett. **571:** 147–153.

Lebel-Hardenack, S., D. Ye, H. Koutnikova, H. Saedler and S. Grant, 1997 Conserved expression of a TASSELSEED2 homolog in the tapetum of the dioecious Silene latifolia and Arabidopsis thaliana. Plant J. **12:** 515–526.

LeClere, S., and B. Bartel, 2001 A library of *Arabidopsis* 35S-cDNA lines for identifying novel mutants. Plant Mol. Biol. **46:** 695–703.

Lei, Z., W. Chen, M. Zhang and J. L. Napoli, 2003 Reduction of *all-trans*-retinal in the mouse liver peroxisome fraction by the short-chain dehydrogenase/reductase RRD: induction by the PPARα ligand clofibrate. Biochemistry **42:** 4190–4196.

Leyser, H. M. O., F. B. Pickett, S. Dharmasiri and M. Estelle, 1996 Mutations in the *AXR3* gene of *Arabidopsis* result in altered auxin response including ectopic expression from the *SAUR-AC1* promoter. Plant J. **10:** 403–413.

Lucas, K. A., J. R. Filley, J. M. Erb, E. R. Graybill and J. W. Hawes, 2007 Peroxisomal metabolism of propionic acid and isobutyric acid in plants. J. Biol. Chem. **282:** 24980–24989.

Marchant, A., J. Kargul, S. T. May, P. Muller, A. Delbarre *et al.*, 1999 AUX1 regulates root gravitropism in *Arabidopsis* by facilitating auxin uptake within root apical tissues. EMBO J. **18:** 2066–2073.

Marchler-Bauer, A., and S. Bryant, 2004 CD-search: protein domain annotations on the fly. Nucleic Acids Res. **32:** 327–331.

Michaels, S. D., and R. M. Amasino, 1998 A robust method for detecting single nucleotide changes as polymorphic markers by PCR. Plant J. **14:** 381–385.

Mursula, A. M., D. M. F. van Aalten, J. K. Hiltunen and R. K. Wierenga, 2001 The crystal structure of [delta]3-[delta]2-enoyl-CoA isomerase. J. Mol. Biol. **309:** 845–853.

Nagpal, P., L. M. Walker, J. C. Young, A. Sonawala, C. Timpte *et al.*, 2000 *AXR2* encodes a member of the Aux/IAA protein family. Plant Physiol. **123:** 563–573.

Neff, M. M., J. D. Neff, J. Chory and A. E. Pepper, 1998 dCAPS, a simple technique for the genetic analysis of single nucleotide polymorphisms: experimental applications in Arabidopsis thaliana genetics. Plant J. **14:** 387–392.

Newman, T., F. J. de Bruijn, P. Green, K. Keegstra, H. Kende *et al.*, 1994 Genes galore: a summary of methods for accessing results from large-scale partial sequencing of anonymous *Arabidopsis* cDNA clones. Plant Physiol. **106:** 1241–1255.

Pellegrini, S., S. Censini, S. Guidotti, P. Iacopetti, M. Rocchi *et al.*, 2002 A human short-chain dehydrogenase/reductase gene: structure, chromosomal localization, tissue expression and subcellular localization of its product. Biochim. Biophys. Acta **1574:** 215–222.

Pickett, F. B., A. K. Wilson and M. Estelle, 1990 The *aux1* mutation of *Arabidopsis* confers both auxin and ethylene resistance. Plant Physiol. **94:** 1462–1466.

Pinfield-Wells, H., E. L. Rylott, A. D. Gilday, S. Graham, K. Job *et al.*, 2005 Sucrose rescues seedling establishment but not ger-

mination of Arabidopsis mutants disrupted in peroxisomal fatty acid catabolism. Plant J. **43:** 861–872.

Poirier, Y., V. D. Antonenkov, T. Glumoff and J. K. Hiltunen, 2006 Peroxisomal [beta]-oxidation: a metabolic pathway with multiple functions. Biochim. Biophys. Acta **1763:** 1413–1426.

Rampey, R. A., S. LeClere, M. Kowalczyk, K. Ljung, G. Sandberg *et al.*, 2004 A family of auxin-conjugate hydrolases that contributes to free indole-3-acetic acid levels during Arabidopsis germination. Plant Physiol. **135:** 978–988.

Reumann, S., C. Ma, S. Lemke and L. Babujee, 2004 AraPerox: a database of putative Arabidopsis proteins from plant peroxisomes. Plant Physiol. **136:** 2587–2608.

Reumann, S., L. Babujee, C. Ma, S. Wienkoop, T. Siemsen *et al.*, 2007 Proteome analysis of Arabidopsis leaf peroxisomes reveals novel targeting peptides, metabolic pathways, and defense mechanisms. Plant Cell **19:** 3170–3193.

Richmond, T. A., and A. B. Bleecker, 1999 A defect in β-oxidation causes abnormal inflorescence development in Arabidopsis. Plant Cell **11:** 1911–1923.

Richmond, T., and S. Sommerville, 2000 Chasing the dream: plant EST microarrays. Curr. Opin. Plant Biol. **3:** 108–116.

Rouse, D., P. Mackay, P. Stirnberg, M. Estelle and O. Leyser, 1998 Changes in auxin response from mutations in an *AUX/IAA* gene. Science **279:** 1371–1373.

Rylott, E. L., C. A. Rogers, A. D. Gilday, T. Edgell, T. R. Larson *et al.*, 2003 *Arabidopsis* mutants in short- and medium-chain acyl-CoA oxidase activities accumulate acyl-CoAs and reveal that fatty acid β-oxidation is essential for embryo development. J. Biol. Chem. **278:** 21370–21377.

Rylott, E. L., P. J. Eastmond, A. D. Gilday, S. P. Slocombe, T. R. Larson *et al.*, 2006 The Arabidopsis thaliana multifunctional protein gene (MFP2) of peroxisomal beta-oxidation is essential for seedling establishment. Plant J. **45:** 930–941.

Schilmiller, A. L., A. J. K. Koo and G. A. Howe, 2007 Functional diversification of acyl-coenzyme A oxidases in jasmonic acid biosynthesis and action. Plant Physiol. **143:** 812–824.

Shafqat, N., J. Shafqat, G. Eissner, H. Marschall, K. Tryggvason *et al.*, 2006 Hep27, a member of the short-chain dehydrogenase/reductase family, is an NADPH-dependent dicarbonyl reductase expressed in vascular endothelial tissue. Cell. Mol. Life Sci. **63:** 1205–1213.

Stasinopoulos, T. C., and R. P. Hangarter, 1990 Preventing photochemistry in culture media by long-pass light filters alters growth of cultured tissues. Plant Physiol. **93:** 1365–1369.

Theodoulou, F. L., K. Job, S. P. Slocombe, S. Footitt, M. Holdsworth *et al.*, 2005 Jasmonic acid levels are reduced in COMATOSE ATP-binding cassette transporter mutants: implications for transport of jasmonate precursors into peroxisomes. Plant Physiol. **137:** 835–840.

Timpte, C., A. K. Wilson and M. Estelle, 1994 The *axr2–1* mutation of *Arabidopsis thaliana* is a gain-of-function mutation that disrupts an early step in auxin response. Genetics **138:** 1239–1249.

van der Krieken, W. M., J. Kodde, M. H. M. Visser, D. Tsardakas, A. Blaakmeer *et al.*, 1997 Increased induction of adventitious rooting by slow release auxins and elicitors, pp. 95–104 in *Biology of Root Formation and Development*, edited by A. Altman and Y. Waisel. Plenum Press, New York.

Wain, R. L., and F. Wightman, 1954 The growth-regulating activity of certain ω-substituted alkyl carboxylic acids in relation to their β-oxidation within the plant. Proc. R. Soc. Lond. Ser. B **142:** 525–536.

Wolf, G., 1984 Multiple functions of vitamin A. Physiol. Rev. **64:** 873–936.

Wong, B. J., and J. A. Gerlt, 2004 Evolution of function in the Crotonase superfamily: (3S)-methylglutaconyl-CoA hydratase from Pseudomonas putida. Biochemistry **43:** 4646–4654.

Woodward, A. W., and B. Bartel, 2005a The *Arabidopsis* peroxisomal targeting signal type 2 receptor PEX7 is necessary for peroxisome function and dependent on PEX5. Mol. Biol. Cell **16:** 573–583.

Woodward, A. W., and B. Bartel, 2005b Auxin: regulation, action, and interaction. Ann. Bot. **95:** 707–735.

Zhang, D., W. Yu, B. V. Geisbrecht, S. J. Gould, H. Sprecher *et al.*, 2002 Functional characterization of delta 3,delta 2-enoyl-CoA isomerases from rat liver. J. Biol. Chem. **277:** 9127–9132.

Zimmermann, P., M. Hirsch-Hoffmann, L. Hennig and W. Gruissem, 2004 GENEVESTIGATOR: Arabidopsis microarray database and analysis toolbox. Plant Physiol. **136:** 2621–2632.

Zolman, B. K., and B. Bartel, 2004 An *Arabidopsis* indole-3-butyric acid-response mutant defective in PEROXIN6, an apparent ATPase implicated in peroxisomal function. Proc. Natl. Acad. Sci. USA **101:** 1786–1791.

Zolman, B. K., A. Yoder and B. Bartel, 2000 Genetic analysis of indole-3-butyric acid responses in *Arabidopsis thaliana* reveals four mutant classes. Genetics **156:** 1323–1337.

Zolman, B. K., M. Monroe-Augustus, B. Thompson, J. W. Hawes, K. A. Krukenberg *et al.*, 2001a *chy1*, an *Arabidopsis* mutant with impaired β-oxidation, is defective in a peroxisomal β-hydroxyisobutyryl-CoA hydrolase. J. Biol. Chem. **276:** 31037–31046.

Zolman, B. K., I. D. Silva and B. Bartel, 2001b The Arabidopsis *pxa1* mutant is defective in an ATP-binding cassette transporter-like protein required for peroxisomal fatty acid β-oxidation. Plant Physiol. **127:** 1266–1278.

Zolman, B. K., M. Monroe-Augustus, I. D. Silva and B. Bartel, 2005 Identification and functional characterization of Arabidopsis PEROXIN4 and the interacting protein PEROXIN22. Plant Cell **17:** 3422–3435.

Zolman, B. K., M. Nyberg and B. Bartel, 2007 IBR3, a novel peroxisomal acyl-CoA dehydrogenase-like protein required for indole-3-butyric acid response. Plant Mol. Biol. **64:** 59–72.

Communicating editor: D. Voytas